Defence Science Journal, Vol. 69, No. 1, January 2019, pp. 46-52, DOI : 10.14429/dsj.69.12821

Effect of Formaldehyde to Phenol Ratio in Phenolic Beads on Pore Structure, Adsorption and Mechanical Properties of Activated Carbon Spheres

Arjun Singh[@,*], Sanjeevan Aggrawal[#], and Darshan Lal[#]

[@]*DRDO-Terminal Ballistics Research Laboratory, Chandigarh - 160 030, India*
[#]*DRDO-Defence Materials and Stores Research and Development Establishment, Kanpur - 208 013, India*
[*]*E-mail: arjunsngh@yahoo.com*

ABSTRACT

Phenolic beads (PBs) prepared from different formaldehyde to phenol (F/P) molar ratios were used as polymeric precursor for activated carbon. Activated carbon spheres (ACSs) have been produced from PBs via the physical activation process using carbon dioxide (CO_2) as activating agent at 950 °C for different burn-off. The prepared ACSs were investigated for nitrogen adsorption, surface morphology and compressive strength by means of BET surface area analyser, scanning electron microscopy (SEM) and carbon and sphere tester techniques. The results indicated that the effects of F/P ratio observed, especially variation in the adsorption and mechanical properties. It was found that ACSs obtained from F/P ratio one showed the superior adsorption properties, possessed a high BET surface area in a range of 836 $m^2\ g^{-1}$ to 3694 $m^2\ g^{-1}$ with high pore volume (0.47 $cm^3\ g^{-1}$ - 2.47 $cm^3\ g^{-1}$) and 73-97 per cent microporosity. The BET surface area and pore volume increased, while the microporosity gradually decreased, with increasing the extent of burn-off. Compressive strength decreased with increasing F/P ratio as well as the extent of burn-off. ACSs upheld improved compressive strength (from 160 N mm^{-2} to 9 N mm^{-2}) than those obtained from F/P ratio 2 and 3 in PBs. SEM studies of ACSs demonstrated well developed pore structure.

Keywords: Phenolic beads; Activated carbon spheres; Physical activation; Mechanical; Adsorption properties

1. INTRODUCTION

Activated carbons have been produced from natural and polymeric precursors by physical and chemical activation processes[1-4]. They are used as a adsorbent material in wide range of applications including gas separation, hydrogen storage, water purification, energy storage, which depends on adsorption properties and pore structure[5,6]. The type of porosity depends on precursor, activation methods and processing conditions. Activated carbons in spherical form are an attractive and superior adsorbent than other forms especially powder and granular due to low ash content, smooth surface, good fluidity, well developed micropores structure, high adsorption properties and reasonable mechanical strength[7-18].

Recently, activated carbon spheres (ACSs) have been prepared from various precursor materials by means of physical and chemical methods. Recently, they are used as strategic adsorbent materials for nuclear, chemical and biology (NBC) protective clothing for removal of toxic substances[3]. It possessed the excellent durability and no abrasion force due to hard beads. For chemical protective clothing, they are permanently fixed on a textile fabric by supporting base. The application of ACSs mainly depends on pore size and pore size distribution which are generally classified into three types namely micropores (size less than 2 nm), mesopores (2 nm to 50 nm) and macropores (more than 50 nm). The meso- and micro-pores are generally contributed to adsorption, while macro-pores are act as conducts for passage for adsorbent materials.

Many studies have been reported on ACSs with high adsorption capacity, but poor mechanical strength for application of protection against toxic substances. ACSs produced from novolac-type phenolic resin by steam activation have been shown low S_{BET} (919 m^2g^{-1}), poor mechanical strength and mesoporous in nature due to cracks on the surface[9,19]. Yang[9], *et al*. have been reported ACSs from novolac-type phenolic resin with S_{BET} of 1663 $m^2\ g^{-1}$ and 37 per cent mesoporosity, resulting a high degree of burn-off 62 per cent. ACSs produced from novolac-type PBs by supercritical water have been possessed S_{BET} of 919 m^2g^{-1} with 17 per cent mesoporosity, resulting a degree of carbon burn-off 50.8 per cent. They have also been produced from polystyrene sulphonate beads with S_{BET} greater than 1200 $m^2\ g^{-1}$ with low mechanical strength.

One way is to tune its chemical structure of phenolic resins by changing monomers molar ratio. It has been investigated that the structure of the precursor has been affected porosity of resulting carbons[21]. The reaction parameters such as temperature, time[22], type of catalyst[23], pH[24] initial formaldehyde to phenol (F/P) molar ratio[25-27] have been strongly affected the properties of phenolic resins. Among these parameters, initial F/P molar ratio plays an important role in the molecular structure or the configuration of the beads[26,27]. Manfredei[25], *et al.* investigated that the molecular structure and other

Received : 20 March 2018, Revised : 12 November 2018
Accepted : 13 December 2018, Online published : 10 January 2019

properties have been influenced by molar ratio of phenol and formaldehyde.

In the present work, an effort is made to prepare ACSs from phenolic beads (PBs) with high adsorption capacity and high mechanical strength by changing F/P ratio in PBs. On other hand, effects of F/P ratio in PBs on pore structure, adsorption properties and mechanical strength of ACSs are investigated which are least reported in the literature. The resole type PBs are prepared from different F/P ratio by suspension polymerisation technique. PBs are carbonised followed by activation with CO_2 as activating agent under nitrogen atmosphere. The adsorption and mechanical properties of ACSs are studied using different analytical techniques.

2. EXPERIMENTAL AND METHODS

2.1 Materials

For synthesis of phenolic beads (PBs), phenol was received from Ranbaxy Laboratories Ltd, India. Aqueous formaldehyde solution LR grade (37-41 % w/v), poly(vinyl alcohol) (PVA) (mol. wt. 125,000) as stabilising agent, and hexamethylene tetramine (HMTA) LR grade as curing agent were received from s-d fine Chem. Ltd, India. Triethyleamine (TEA) as catalyst was received from Eeastgate White Lund Morecaube, England. Acetone (AR grade) was obtained from Samir Tech-Chem Pvt. Ltd, India.

2.2 Preparation of PBs

Resole type-PBs were synthesised by suspension polymerisation method[28,29] using a water as aqueous medium. The polymerisation reaction of phenol with formaldehyde was performed in a round bottomed reaction vessel fitted with thermocouple condenser and mechanical agitator in the presence of TEA as catalyst. In this reaction, phenol and formaldehyde were mixed at different molar ratios (i.e. 1:1, 1:2 and 1:3 of phenol and formaldehyde respectively by mole) in a reaction vessel containing 230 ml of water in a presence of TEA as catalyst. Then, 5.0 wt % stabilising agent (PVA) was added to the above mixture at temperature of 96±1 ^{o}C with agitation rate of 475 rpm for 40 min. At the end of reaction, 3.5 wt.% HMTA as curing agent was added to above-mentioned solution and synthesis continued for 4 h. Finally, the solution was filtered and dried to obtain PBs.

2.3 Preparation of ACSs

PBs prepared from different F/P molar ratio were used as polymeric precursor for preparation of ACSs. ACSs were prepared by carbonising of PBs followed by activation with CO_2 as activating agent under nitrogen atmosphere. The carbonisation process[14] was carried in a vertical tubular furnace at 25 °C to 900 °C at a heating rate of 10 °C min^{-1} under nitrogen atmosphere. The resulting material was carried out for activation process (burn-off) with CO_2 as activating agent in a same reactor. The activation process was typically thermal process conducted at high temperature 950 °C using CO_2 as activating agent for different activation time. The development of porosity was increased with burn-off by removing volatile material from the solid carbons. ACSs samples were prepared from PBs at 950 °C at different extent of burn-off as following; ACS_{27}, ACS_{58}, and ACS_{86} samples from PBs having F/P ratio 1 were obtained at 27 per cent, 58 per cent, and 86 per cent burn-off, respectively. ACS_{56}, ACS_{78} and ACS_{85} samples were obtained from PBs having F/P ratio 2 at different extent of burn-off 56 per cent, 78 per cent, and 85 per cent, respectively and ACS_{66}, ACS_{74} and ACS_{88} samples were obtained from PBs having F/P ratio 3 for different extent of burn-off 66 per cent, 74 per cent, and 88 per cent, respectively.

2.4 Measurements and Characterisation

Nitrogen adsorption isotherms were measured at -196 °C using a nitrogen molecule as adsorbent by means of a surface area analyser as supplied by quantachrome autosorbed. All samples were degassed at 250 °C for 5 h before nitrogen adsorption measurement. Brunauer–Emmett–Teller (BET) model[30,31] was used to fit the nitrogen adsorption isotherms and assess the specific surface area (S_{BET}) of ACSs. Dubinin-Radushkevitch (DR) model[32] was applied to determine micropore volume (V_{micro}) of ACSs. Pore volume (V_{pore}) of the test sample was calculated from nitrogen adsorption isotherm data. V_{pore} was estimated the amount of nitrogen adsorbed at a relative pressure of 0.98[33]. Pore size distribution of V_{meso} was investigated using a Barrett, Joyner, and Halenda (BJH) method[34]. Average pore size (D_{av}) was determined by four time total pore volume of ACSs divided by its corresponding surface area. Yield percentage was calculated by weighing method. Surface morphology and internal pore structure were studied using a scanning electron microscopy (SEM) as supplied by Carlo ZEISS. Beads were broken before SEM measurement and sputter coated with gold before analysis. Compressive strength was investigated using a Carbon and Sphere Tester (ASTM C-695) using at least 10 beads for each sample and average value of compressive strength was reported.

3. RESULTS AND DISCUSSION

3.1 PBs Analysis

Size of PBs in the range of 0.2 mm - 1.2 mm was taken for ultimate and proximate analysis. Table 1 shows the results of ultimate and proximate analysis of PBs. The results showed that carbon content decreased with increase in F/P molar ratio, while oxygen content increased with increasing the F/P ratio due to the formation of ether linkage in the phenolic resin structure network[28]. Residual matter which was left after completion of pyrolysis process was also determined. Proximate analysis reveals that it contains 39-41 per cent of volatile matter and free from ash content.

3.2 ACS from CO_2 Gasification

Figures 1(a)-1(c) shows adsorption isotherms of (a) ACS_{27}, ACS_{58}, ACS_{86}; (b) ACS_{56}, ACS_{78}, ACS_{85}; (c) ACS_{56}, ACS_{78}, ACS_{85} samples obtained from different F/P ratio in PBs at 77 K for different extent of burn-off, respectively. Desorption isotherms were also recorded under same experimental conditions which are not shown in the figure. It is observed that adsorption isotherms of ACS_{27} and ACS_{58} samples are very sharp at low relative pressure, thereafter plateaus are fairly horizontal, indicating mainly microporous carbon structure. While, adsorption isotherm of ACS_{86} is shifted from Type I

Table 1. The results of ultimate and proximate analysis of PBs

F/P (mole)	Ultimate (wt. %)				Proximate (wt. %)			
	Carbon	Hydrogen	Nitrogen	Oxygen	Moisture	Volatile matter	Fixed carbon	Ash
1	69.1	6.7	1.2	22.4	4.5	40.8	54.7	0.0
2	68.4	6.3	1.5	23.5	5.1	39.8	55.1	0.0
3	66.0	6.5	1.7	25.7	5.1	39.2	55.7	0.0

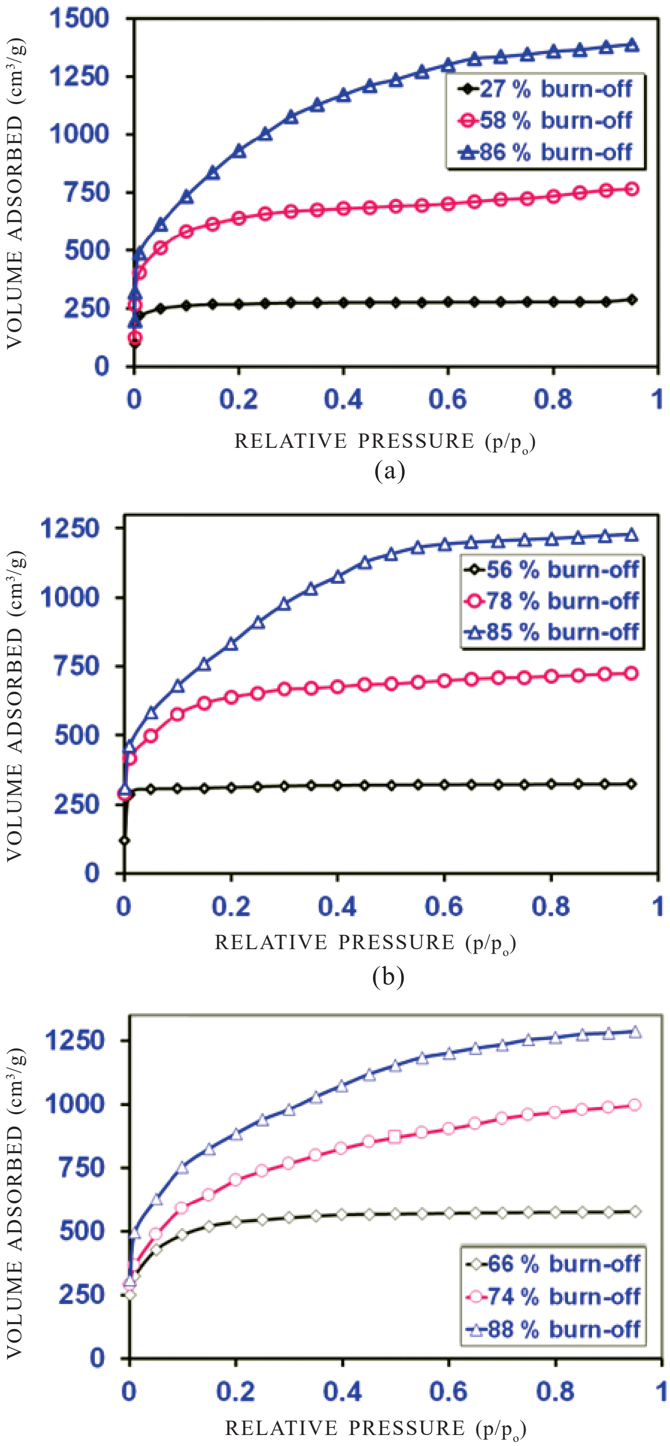

(a)

(b)

(c)

Figure 1. Adsorption isotherms of ACSs obtained from PBs having: (a) F/P = 1, (b) 2, and (c) 3 at activation temperature 950 °C with CO_2 gasification at different burn-off.

to mixture of Type I and Type IV adsorption isotherm at high relative pressure. It indicates that ACSs possess meso- and micro-pore structure according to Brunauer, Deming, Deming and Teller (BDDT) classification[35].

The adsorption isotherms for ACS_{56} and ACS_{66} samples obtained from F/P ratio 2 and 3, respectively (Figs. 1(b)&1(c)) are the characteristic of Type I isotherm according to BDDT classification. However, N_2 adsorption isotherms of ACS_{78}, ACS_{85}, ACS_{74}, and ACS_{88} samples increased with increasing the relative pressure, representing Type I and Type IV adsorption isotherms. This confirms that the prepared ACSs possess both meso- and micro-pores type carbon structure at high burn-off according to BDDT classification.

Detailed characteristics of the adsorption properties along with pore diameter are summarised in Table 2. It was observed that S_{BET} and V_{pore} of ACSs from F/P ratio 1 and 2 increased with increasing extent of burn-off. The S_{BET} increased from 886 m^2g^{-1} to 3685 m^2g^{-1} when burn off increased from 28 to 86 per cent, which is a higher value than those reported in the literature[15,17,36]. ACSs are mainly microporous in nature and the microporosity gradually decreased with increasing the extent of burn-off. This is attributed the fact that the CO_2 reacted with carbon atoms, resulting open up closed pores and enlarging of the existing micropore. In case of ACSs from F/P ratio 3, S_{BET} and V_{pore} initially increased to attain maximum value, thereafter decreased with extent of burn-off. This indicated that adsorption properties of ACSs significantly reduced than those ACSs obtained from F/P ratio 1 and 2. The decrease in the adsorption properties was due to breaking of walls of pores during CO_2 gasification, resulting in the large mesopore structure. Yield of ACSs during gasification decreased with extents of burn-off. The decrease in carbon yield is attributed to fast carbon gasification with CO_2.

As far as the effect of F/P ratio is concerned, the slope of adsorption isotherms (plateaus) at high relative pressure relatively found to be increased with increase in F/P ratio in PBs, indicating that the opening of a knee of the isotherms due to widening of pore structure. The adsorption properties including S_{BET} and V_{pore} decreased with increasing F/P ratio in the PBs. The widening of pore structure further confirmed by adsorption data where the microporosity reduced with increasing F/P ratio in the PBs. The decrease in the adsorption properties and microporosity for ACSs from F/P ratio 3 may be caused of high oxygen content in the PBs due to existence of ether linkage. It was reported that oxygen index in the PBs[28] increased with increasing the F/P as shown in Table 1. It is suggested that the pyrolysis during carbonisation of PBs resulting high heat release caused to pore widening with low adsorption properties. It concludes that ACSs prepared from F/P ratio 1 and 2 shows higher adsorption properties and

Table 2. Adsorption properties of ACSs prepared from PBs containing different F/P ratio 1, 2 and 3 at 950 °C with CO_2 gasification at different burn-off

Sample	F/P (mole)	Char burn-off (per cent)	Yield (per cent)	S_{BET} ($m^2\ g^{-1}$)	V_{pore} ($cm^3\ g^{-1}$)	Pore size distribution		D_{av} (A°)
						V_{micro} ($cm^3\ g^{-1}$)	V_{meso} ($cm^3\ g^{-1}$)	
ACS_{27}	1	27	48.3	836	0.47	0.46	0.01	22.5
ACS_{58}		58	23.2	2340	1.67	1.42	0.25	28.5
ACS_{86}		86	7.0	3685	2.47	1.86	0.61	26.8
ACS_{56}	2	56	24.3	1413	0.56	0.53	0.03	15.9
ACS_{78}		78	13.1	2420	1.56	1.24	0.32	25.8
ACS_{85}		85	8.0	3150	2.42	1.43	0.99	30.7
ACS_{66}	3	66	20.1	1230	0.89	0.79	0.10	28.9
ACS_{74}		74	12.3	2040	1.23	0.94	0.29	24.1
ACS_{88}		88	6.7	1380	1.15	0.60	0.65	33.3

contained a large number of original pores than those prepared from F/P ratio 3.

3.3 Pore Size Structure

The microporosity of ACSs is determined by DR equation[32] as shown below

$$W = W_o \exp\left[-\left(RT\log\left(\frac{p_o}{p}\right)/\beta E_o\right)^2\right] \qquad (1)$$

where W represents volume of pores filled, the unit mass of adsorbent ($cm^3\ g^{-1}$) at temperature T and p/p_o. W_o represents the maximum micropore volume of adsorbent. R is gas constant. E_o and β are the characteristics of energy for adsorption and affinity co-efficient for characteristic curves, respectively.

This is equation of straight line in which log(W) and $\log^2(p_o/p)$ are two variables. The total volume of the micropores (W_o) was calculated linear slope DR plots by plotting of log (W) against $\log^2(p_o/p)$. Figure 2 shows DR plots of log(W) against $\log^2(p_o/p)$ for ACSs obtained from F/P ratio 1 in PBs. It was observed that there was linearity over a wide range of the relative pressure, indicating the presence of narrow pores. DR plots also showed an upward derivation at very high relative pressure, indicating excess adsorption of N_2 molecules than expected. This excess adsorption could be best described by capillary condensation in mesopore structure. The microporosity calculated for ACS_{27}, ACS_{58} and ACS_{86} was 97.0 per cent, 79.1 per cent, and 73.5 per cent, respectively. The decrease in microporosity with extent of burn-off can also be seen from DR plots. Similarly, the microporosity calculated from DR equation for ACS_{56} ACS_{78} and ACS_{85} was 95.0 per cent, 79.2 per cent, and 59.2 per cent, respectively. It can be seen that the type of microstructure of carbons depends on monomers ratio of polymeric materials[37].

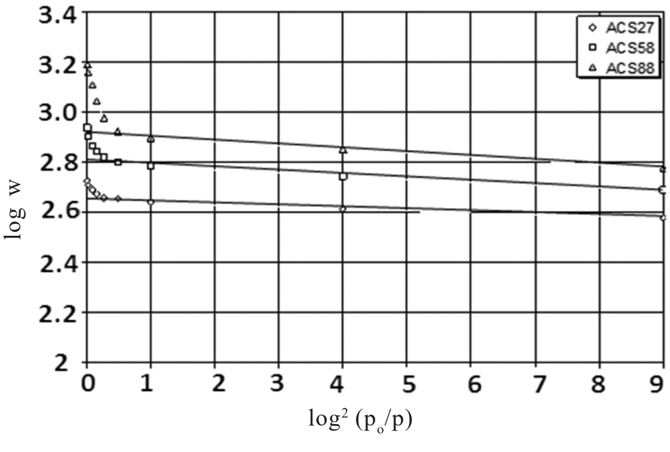

Figure 2. DR plots of ACSs obtained from PBs having F/P ratio 1.

The pore size distribution of ACS_{27}, $ACS_{58,}$ and ACS_{86} samples was also determined by BJH method. Figures 3(a)-3(c) shows mesopore size distribution of ACS_{27}, $ACS_{58,}$ and ACS_{86} samples prepared from F/P ratio 1 at different extent of burn-off. The data obtained for corresponding ACSs samples for pore size distribution are listed in Table 2. It can be seen that the pore size increased with extent of burn-off due to pore widening. ACS_{86} also showed a broad mesopore distribution as accumulate in size in a range of 20 A° - 45 A°.

3.4 Surface Morphology

Figures 4(a)-4(c) shows SEM micrographs of a single bead of ACS_{86}, ACS_{85} and ACS_{88} samples prepared at 950 °C with CO_2 gasification. SEM micrographs provide an important information related to porosity in ACSs. It can be seen that pores are well developed inside carbon structure which are more and less uniform. SEM studies also reveal that pores are relatively small sizes at low burn-off as compared to those developed at high burn-off.

3.5 Compressive Strength of ACSs

Figure 5 shows compressive strength of ACSs prepared from different F/P ratio in PBs at 950 °C with CO_2 gasification for different extent of burn-off. It can be seen that ACSs from F/P ratio 1 showed high compressive strength even at high burn-off. The compressive strength decreased 140 N mm^{-2} to 9 N mm^{-2} when the extent of burn-off increased from 27 per cent to 86 per cent. As far as the effect of F/P ratio is concerned, it can be seen that compressive strength of ACSs obtained from F/P ratio of 1 has a higher than those of ACSs from F/P ratio 2. The compressive strength of ACSs reduced with increasing F/P ratio. It concludes that ACS_{58} sample prepared from F/P ratio 1 show excellent compressive strength as compared to ACSs reported in literature[15,16,20]. In most of studies[20], the compressive strength was significantly dropped even at low surface area due to cracks on the surface of beads.

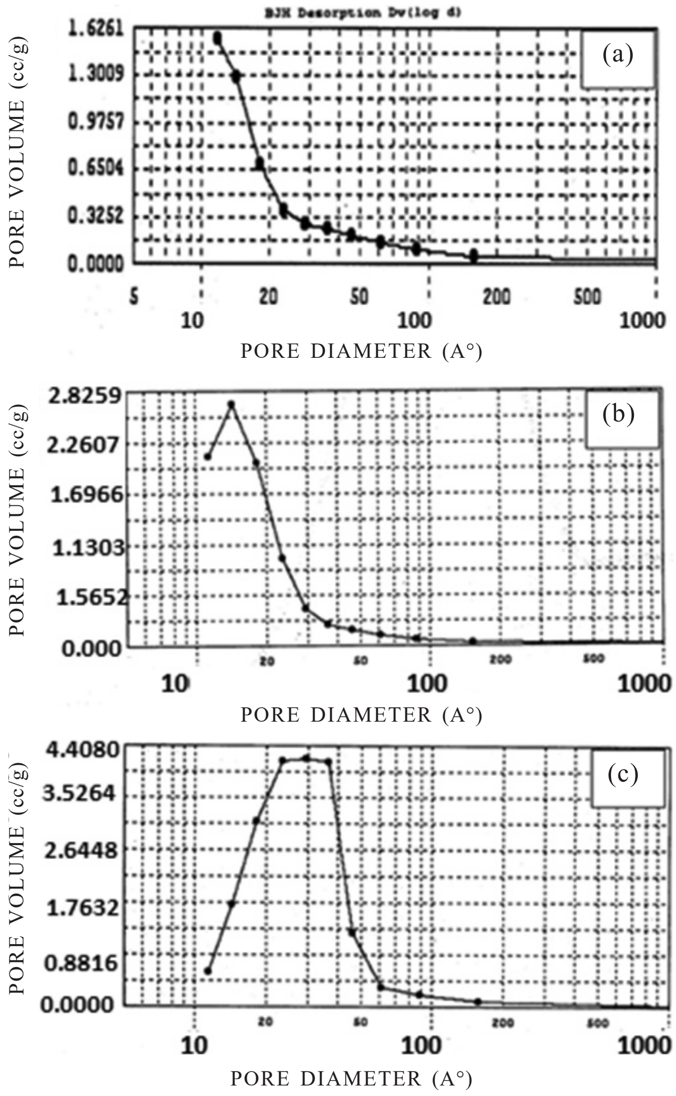

Figure 3. (a)-(c) Pore size distribution of ACSs prepared from PBs having F/P ratio 1 using BJH. method.

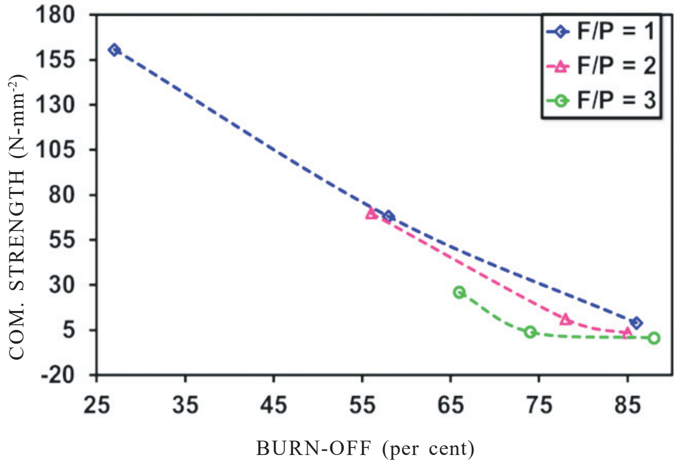

Figure 5. Compressive strength of ACS$_s$ prepared from PBs having different F/P ratio at 950 °C with CO$_2$ gasification for different burn-off.

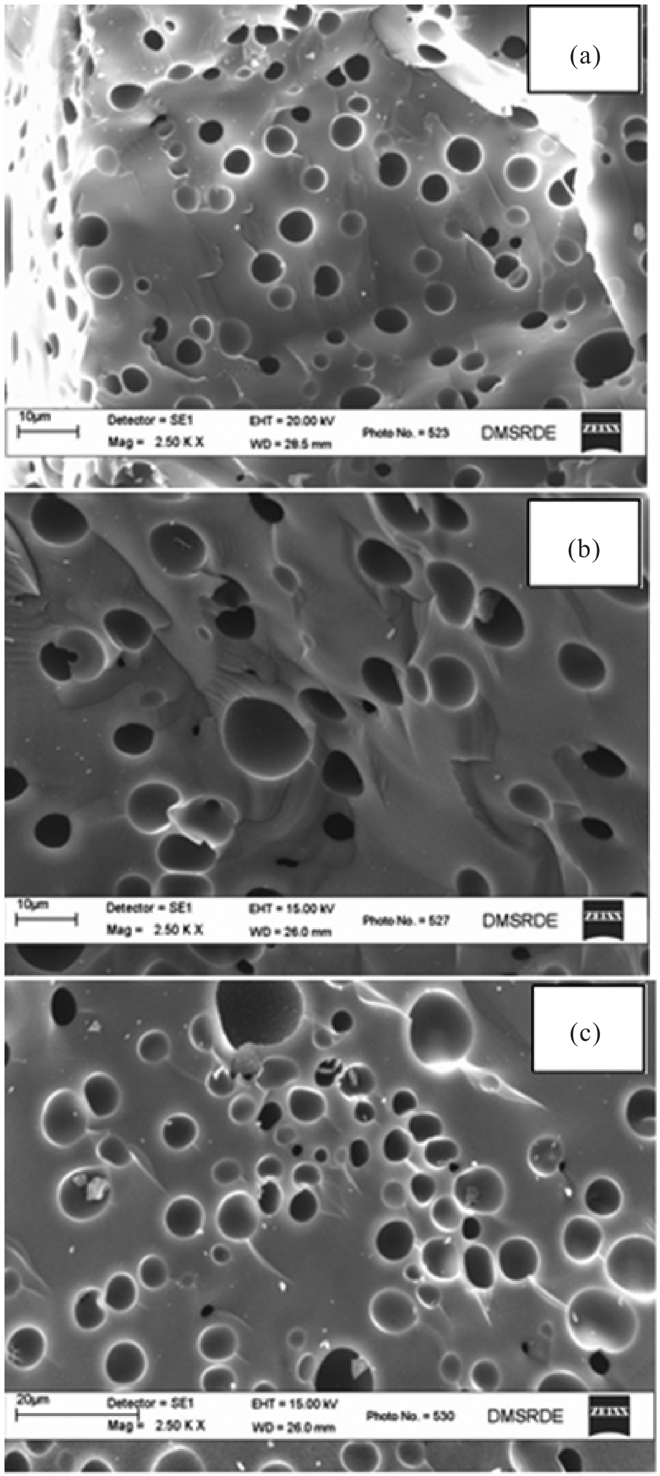

Figure 4. SEM micrographs of (a) ACS$_{86}$, (b) ACS$_{85}$ and (c) ACS$_{88}$ prepared from PBs at 950 °C with CO$_2$ gasification for 86 per cent, 85 per cent and 88 per cent burn-off, respectively.

4. CONCLUSIONS

In the present study, ACSs have been prepared from different F/P ratio in the PBs at 950 °C with CO$_2$ as activating agent at different extent of burn-off. ACSs obtained from F/P ratio 1 in PBs are mainly microporous in nature and the microporosity has gradually reduced from 97.0 per cent to 73.5 per cent when the extent of burn-off varied from 27 per cent to

86 per cent. The S_{BET} and V_{pore} are found to be increased with increase in the extents of burn-off and achieved maximum S_{BET} of 3685 m^2 g^{-1} with V_{pore} of 2.47 cm^3 g^{-1}. It is observed that adsorption properties of ACSs were decreased with increasing F/P molar ratio in PBs. SEM micrographs have shown a well-developed pore structure and no cracks on surface. ACSs obtained from F/P ratio 1 in PBs has demonstrated high adsorption properties, improved compressive strength and better yield than those obtained from F/P molar ratio 2 and 3 in PBs. These materials can be suitable to be a good adsorbent material in many applications.

REFERENCES

1. Bansal, R.C.; Donnet, J. B. & Stoeckli H.F. Activated Carbon. *New York: Marcel Dekker,* 1988, 259-333.
2. Teng, H. & Wang, S. C. Influence of oxidation on the preparation of porous carbons from phenol−formaldehyde resins with KOH activation. *Ind. Eng. Chem. Res.,* 2000, **39**(3), 673-678.
   doi: 10.1021/ie990473i.
3. Thakare, V.B.; Tripathi, N.K.; Singh, V.V.; Sathe, M. & Singh B. Activated Carbon Fabric: An Adsorbent Material for Chemical Protective Clothing. *Def. Sci. J.*, 2018, **68**(1), 83-90.
   doi : 10.14429/dsj.68.11734.
4. Teng, H. & Wang, S.C. Preparation of porous carbons from phenol-formaldehyde resins with chemical and physical activation. *Carbon,* 2000, **38**(6), 817-824.
   doi: 10.1016/S0008-6223(99)00160-8.
5. Sahoo, S. & Ramgopal, M. Experimental studies on an indigenous coconut shell based activated carbon suitable for natural gas storage. *Sadhana,* 2016, **41**, 459-68.
   doi: 10.1007/s12046-016-0483-x.
6. Sharon, M. & Sharon, M. Carbon Nanomaterials: Applications in physico-chemical systems and biosystems. *Def. Sci. J.,* 2008, **58**(4), 460-485.
   doi: 10.14429/dsj.58.1668.
7. Yang, J.B. Preparation structure and properties of phenolic resin-based spherical activated carbon. PhD thesis, Institute of Coal Chemistry. *Chinese Academy Sci. (Chinese),* 1999.
8. Liu, C.; Liang, X. & Liu, X. Wettability modification of pitch-based spherical activated carbon by air oxidation and its effects on phenol adsorption. *Appl. Surf. Sci.,* 2007, **254**, 2659-2665.
   doi: 10.1016/j.apsusc.2007.10.026.
9. Yang, J.; Ling, L. & Liu, L. Preparation and properties of phenolic resin-based activated carbon spheres with controlled pore size distribution. *Carbon* 2002, **40**(6), 911-916.
   doi: 10.1016/S0008-6223(01)00222-6.
10. Liu, Z.; Ling, L. & Qiao, W. Effects of various metals and their loading methods on the mesopore formation in pitch-based spherical activated carbon. *Carbon* 1999, **37**(8), 1333-1335.
    doi: 10.1016/j.jhazmat.2010.03.073.
11. Singh, A. & Lal, D. Influence of heating rate and temperature on carbon structure and porosity of activated carbon spheres from resole-type phenolic beads. *Carbon Let.,* 2009, **10**(2), 181-189.
12. Huang, F. C.; Lee, C. K.; Han, Y. L.; Chao, W. C. & Chao, H. P. Preparation of activated carbon using micro-nano carbon spheres through chemical activation. *J. Taiwan Inst. Chem. Eng*., 2014, **45**, 2805–2812.
    doi: 10.1016/j.jtice.2014.08.004
13. Wang, Q.; Liang, X. Y.; Zhang, R.; Liu, C. J.; Liu, X. J.; Qiao, W. M.; Zhan, L. & Ling, L. C. Preparation of polystyrene-based activated carbon spheres and their adsorption of dibenzothiophene. *New Carbon Mat.,* 2009, **24**(1), 55-60.
14. Singh, A. & Lal, D. Microporous activated carbon spheres prepared from resole-type crosslinked phenolic beads by physical activation. *J. Appl. Polym. Sci.,* 2008, **110**, 3283-3291.
    doi: 10.1002/app.28846.
15. Singh, A. & Lal, D. Preparation and characterization of activated carbon spheres from polystyrene sulphonate beads by steam and carbon dioxide activation. *J. Appl. Polym. Sci*., 2010, **115**, 2409-2415.
    doi: 10.1002/app.31340.
16. Wickramaratne, N. P. & Jaroniec, M. Activated carbon spheres for CO_2 adsorption. *ACS Appl. Mater. Interf.,* 2013, **5**(5), 1849-1855.
    doi: 10.1021/am400112m.
17. Yang, Y.; Shi, Q.; Feng, J.; Shu, X. & Feng J. Preparation and antibacterial properties of an activated carbon sphere–quaternary phosphonium salt composite. *RSC Advances,* 2014, 4, 50708-50712.
    doi:10.1039/C4RA07282K.
18. Liu., Z.; Ling, L. & Qiao, W. Effect of hydrogen on the mesopore development of pitch-based spherical activated carbon containing iron during activation by steam. *Carbon,* 1999, **37**(12), 2063-6.
    doi: 10.1016/S0008-6223(99)00058-5.
19. Huanga, F. C.; Leeb, C. K.; Chaod, W. C. & Chaoe, H. P. Preparation of activated carbon using micro-nano carbon spheres through chemical activation. *J. Taiwan Inst. Chem. Eng.,* 2014, **5**(5), 2805-2812.
    doi: 10.1016/j.jtice.2014.08.004.
20. Cai, Q.; Huang, Z. H.; Kang, F. & Yang, J. B. Preparation of activated microspheres from phenolic resin by supercritical water activation. *Carbon,* 2004, **42**(4), 775-83.
    doi: 10.1016/j.carbon.2004.01.042.
21. Laine, J. & Yunes, S. Effect of the preparation method on the pore size distribution of activated carbon from coconut shell. *Carbon,* 1992, **30**, 601-04.
    doi: 10.1016/0008-6223(92)90178-Y.
22. Grenier-Loustalot, M. F.; Larroque, S.; Grande, D. & Grenier, P. Phenolic resins: 2. Influence of catalyst type on reaction mechanisms and kinetics. *Polym.,* 1996, **37**, 1363-70.
    doi: 10.1016/0032-3861(96)81133-5.
23. Astarloa-Aierbe, G.; Echeverrı, J. M.; Vazquez, A. & Mondragon I. Influence of the amount of catalyst and initial pH on the phenolic resol resin formation. *Polymer*,

2000, **41**, 3311-115.
doi: 10.1016/S0032-3861(99)00519-4.

24. Li, G.F.; Huang, Y. & Chen, C.H. The influence of formaldehyde/phenol ratio on properties of foamable phenolic resin and phenolic foam. *Adv. Mater. Res.,* 2011, **523**, 250– 253.
doi: 10.4028/www.scientific.net/AMR.250-253.523.
25. Manfredi, L. B.; de la Osa, O.; Galego, F. N. & Vazquez A. Influence of the amount of catalyst and initial pH on the phenolic resol resin formation. *Polym.,* 1999, **40**, 3867-75.
doi: 10.1021/ie010610n.
26. Astarloa-Aierbe, G.; Echeverrı, J. M.; Martin, M. D.; Etxeberria, A. M. & Mondragon, I. Influence of the amount of catalyst and initial pH on the phenolic resol resin formation. Polym., 2000, **41**, 6797-6802.
doi: 10.1016/S0032-3861(00)00044-6.
27. Hu, X. M.; Zhao, Y. Y. & Cheng, W. M. Effect of formaldehyde/phenol ratio (F/P) on the properties of phenolic resins and foams synthesized at room temperature. *Polym Compo.,* 2015, **36**, 1531-1540.
doi: 10.1002/pc.23060.
28. Singh, A.; Yadav, R. K. & Srivastava, A. Synthesis of resole-type phenolic beads from phenol and formaldehyde by suspension polymerization technique. *J. Appl. Polym. Sci.,* 2009, **112**, 1005-11.
doi: 10.1002/app.29480.
29. Singh, A. & Lal, D. Effect of reaction parameters on the particle sizes of cross-linked spherical phenolic beads by suspension polymerization of phenol and formaldehyde. *J Appl. Polym. Sci.,* 2006, **100**, 2323-30.
doi: 10.1002/app.22995.
30. Gregg, S. & Sing, K.S.W. Adsorption, Surface area and porosity. London, Academic Press*,* 1982, 42-112.
31. Gregg, S. & Sing, K.S.W. Adsorption, surface area and porosity. *London, Academic Press,* 1982*,* 195-257.
32. Dubinin, M.M. Fundamentals of the theory of adsorption in micropores of carbon adsorbents. Carbon, 1998, **27**, 457-467.
33. Freeman, J.J.; Gimblett, F.G.R. & Sing, K.C.W. Studies of activated charcoal cloth. V. Modification of pore structure by impregnation with certain transition metal salts and oxo-complexes. *Carbon,* 1989, **27**(1), 85-93.
doi: 10.1016/0008-6223(89)90160-7.
34. Barrett, E.P.; Jaoyner, L.G. & Halenda, P.P. The determination of pore volume and area distributions in porous substance. I. Computations from nitrogen isotherms. J *Am. Chem. Soc.,* 1951, **73**, 373-80.
doi: 10.1021/ja01145a126.
35. Brunauer, S.; Demnig, L.S.; Demnig, W.S. & Teller, E. On a theory of the Van der Waals adsorption of gases. *J. Am. Chem. Soc.,* 1940, **62**, 1723-32.
doi: 10.1021/ja01864a025.
36. Yenisoy-Karakas, S.S.; Aygun, A.; Gunes, M. & Tahtasakal, E. Physical and chemical characteristics of polymer- based spherical activated carbons and its ability to adsorb organics. *Carbon,* 2004, **42**, 477.
doi: 10.1016/j.carbon.2003.11.019.
37. Linares, C.D.; Lillo, R.M.A.; Cazorla, A.D. & Linarres, S.A. Preparation of activated carbons from Spanish anthracite: I. Activation by KOH. *Carbon,* 2001, **39**, 741-49.
doi: 10.1016/S0008-6223(00)00185-8.

CONTRIBUTORS

Dr Arjun Singh received his PhD in Chemistry from Panjab University, Chandigarh. Presently, he is working as Scientist in DRDO-Terminal Ballistics Research Laboratory, Chandigarh. He has research experience in fluoropolymer, phenolic resins, activated carbon, high energetic materials, synthesis of energetic composite, etc.
In the current study, he designed the experiments and contributed by preparation of ACSs and evaluation of compressive strength. He had also interpreted of adsorption data and drafted the manuscript.

Mr Sanjeevan K. Agrawal received his MSc in Chemistry and working as Technical Officer at the DRDO-Defence Materials & Stores and Research and Development Establishment, Kanpur. His areas of interest are scale of activated carbon spheres, characterisation of porous carbons and test methodologies for chemical protective suit.
In the present work, he contributed the characterisation of activated carbon spheres for adsorption properties by using surface area analyser.

Mr Darshan Lal received his BE (Chemical Engineering) and he is working as Scientist 'F' at the DRDO-Defence Materials and Stores Research and Development Establishment, Kanpur. His areas of research are scale up of activated carbon spheres, production of carbon materials, development of chemical protective suit and process development of activated carbons.
In the present study, he was involved in overall guidance, critical suggestions and approval of manuscript.